

## Research Article

# Axisymmetric Stagnation Flow of a Micropolar Nanofluid in a Moving Cylinder

**S. Nadeem,<sup>1</sup> Abdul Rehman,<sup>1</sup> K. Vajravelu,<sup>2</sup>  
Jinho Lee,<sup>3</sup> and Changhoon Lee<sup>4</sup>**

<sup>1</sup> Department of Mathematics, Quaid-i-Azam University, Islamabad 44000, Pakistan

<sup>2</sup> Department of Mathematics, University of Central Florida, Orlando, FL 32816, USA

<sup>3</sup> School of Mechanical Engineering, Yonsei University, Seoul 120-749, Republic of Korea

<sup>4</sup> Department of Computational Sciences and Engineering, Yonsei University,  
Seoul 120-749, Republic of Korea

Correspondence should be addressed to S. Nadeem, snqau@hotmail.com

Received 5 August 2011; Accepted 1 November 2011

Academic Editor: J. Jiang

Copyright © 2012 S. Nadeem et al. This is an open access article distributed under the Creative Commons Attribution License, which permits unrestricted use, distribution, and reproduction in any medium, provided the original work is properly cited.

An analysis is carried out for axisymmetric stagnation flow of a micropolar nanofluid in a moving cylinder with finite radius. The coupled nonlinear partial differential equations of the problem are simplified with the help of similarity transformations and the resulting coupled nonlinear differential equations are solved analytically by homotopy analysis method (HAM). The features of the flow phenomena, inertia, heat transfer, and nanoparticles are analyzed and discussed.

## 1. Introduction

During the past years, the study of stagnation flows has become more and more important because of their applications in engineering and technology. Hiemenz [1] first discussed the steady flow of a Newtonian fluid impinging orthogonally on an infinite flat plate. Later on, a large number of papers have been done on orthogonal, nonorthogonal, and axisymmetric stagnation flows. Some important studies on the topic include references [2–10].

A large amount of literature is available on the viscous theory. However, only a limited attention has been given to the study of non-Newtonian fluids. There are two major reasons responsible for this. The main reason is that the additional nonlinear terms arising in the equation of motion rendering the problem more difficult to solve [11]. The second reason is that a universal non-Newtonian constitutive relation that can be used for all fluids and flows are not available. The study of non-Newtonian fluids has many applications in various industries, such as nuclear paints, physiology, biomechanics, chemical engineering, and technology. There are many non-Newtonian fluid models. However, Eringen [12] proposed

the theory of micropolar fluid that is capable to describe practical fluids by taking into account the effects arising from local structure and micromotion of the fluid elements. The study has attracted many researchers to investigate the non-Newtonian fluids with various aspects.

Recently, the study of convective transport of nanofluids has gained considerable importance due to its applications. According to Khan and Pop [13] most of the conventional transfer fluids like oil, water, and ethylene glycol are poor heat transfluids because the thermal conductivity of these fluids plays an important role on the heat transfer coefficient between the heat transfer medium and heat transfer surface. The importance of these nanofluids has been discussed by Choi [14]. Kuznetsov and Nield [15] have studied the thermal instability in a porous medium layer saturated by nanofluids.

Keeping the above importance in mind, the aim of the present work is to discuss the axisymmetric stagnation flow of a micropolar nanofluid flow in a moving cylinder. To the best of the authors' knowledge, no attempt has been made in this direction. The governing equations of the micropolar fluid along with heat transfer and nanoparticle equation are simplified by applying suitable similarity transformations and then the reduced highly nonlinear-coupled equations are solved analytically with the help of homotopy analysis method. The convergence of the HAM solution and the physical behavior of pertinent parameters of the problem are discussed through graphs.

## 2. Formulation

Let us consider an incompressible flow of a micropolar nanofluid between two cylinders such that the flow is axisymmetric about  $z$ -axis. The inner cylinder is of radius  $R$  rotating with angular velocity  $\Omega$  and moving with velocity  $W$  in the axial  $z$ -direction. The inner cylinder is enclosed by an outer cylinder of radius  $bR$ . Further, the fluid is injected radially with velocity  $U$  from the outer cylinder towards the inner cylinder. The geometry of the problem is shown in Figure 1. The governing equations of motion and microinertia in the presence of nanoparticles and the heat transfer are

$$r\omega_z + (ru)_r = 0, \quad (2.1)$$

$$\rho \left( uu_r + wu_z - \frac{v^2}{r} \right) = -p_r + (\mu + k^*) \left( u_{rr} + \frac{1}{r}u_r + u_{zz} - \frac{u}{r^2} \right) - k^*N_z^*, \quad (2.2)$$

$$\rho \left( uv_r + wv_z + \frac{uv}{r} \right) = (\mu + k^*) \left( v_{rr} + \frac{1}{r}v_r + v_{zz} - \frac{v}{r^2} \right), \quad (2.3)$$

$$\rho(uw_r + ww_z) = -p_z + (\mu + k^*) \left( w_{rr} + \frac{1}{r}w_r + w_{zz} \right) + k^* \left( N_r^* + \frac{1}{r}N^* \right), \quad (2.4)$$

$$\rho j(uN_r^* + wN_z^*) = -2kN^* + k^*(u_z - w_r) + \gamma \left( N_{rr}^* + \frac{1}{r}N_r^* + N_{zz}^* - \frac{1}{r^2}N^* \right), \quad (2.5)$$

$$\rho c_p(u\sigma_r + w\sigma_z) = k \left( \sigma_{rr} + \frac{1}{r}\sigma_r + \sigma_{zz} \right) + \rho^* c_p^* \left[ D_B(\phi_r\sigma_r + \phi_z\sigma_z) + \frac{D_T}{\sigma_1}(\sigma_r^2 + \sigma_z^2) \right], \quad (2.6)$$

$$u\phi_r + w\phi_z = D_B \left( \phi_{rr} + \frac{1}{r}\phi_r + \phi_{zz} \right) + \frac{D_T}{\sigma_1} \left( \sigma_{rr} + \frac{1}{r}\sigma_r + \sigma_{zz} \right), \quad (2.7)$$

where (2.1) is the continuity equation, (2.2)–(2.4) are the  $r$ ,  $\theta$  and  $z$  components of momentum equation, (2.4)–(2.6) are the angular momentum, temperature, and nanoparticle concentration equations. Note that neglecting microrotation and nanoparticle concentration, the remaining system would be that solved by Hong and Wang [16]. In the above equations ( $u, v, w$ ) are the velocity components along the  $(r, \theta, z)$  axes,  $N^*$  is the angular microrotation momentum,  $\mu$  is the dynamic viscosity,  $k^*$  is the vortex viscosity,  $j$  is the microrotation density,  $\gamma$  is the micropolar constant,  $\rho$  is density,  $c_p$  is the specific heat at constant pressure,  $\nu$  is the kinematic viscosity,  $\sigma$  is temperature,  $k$  is the thermal conductivity,  $\phi$  is the nanoparticle volume fraction,  $\rho^*$  is the nanoparticle mass density,  $c_p^*$  is the effective heat of the nanoparticle material,  $D_B$  is the Brownian diffusion coefficient,  $D_T$  is the thermophoretic diffusion coefficient, and  $p$  is pressure.

Let us define the following similarity transformations and nondimension variables as

$$\begin{aligned} u &= -\frac{Uf(\eta)}{\sqrt{\eta}}, & v &= \Omega ah(\eta), & w &= 2Uf'(\eta)\xi + Wg(\eta), \\ N^* &= 2\frac{U}{R}M(\eta)\xi + \frac{W}{R}N(\eta), \\ \theta &= \frac{\sigma - \sigma_1}{\sigma_b - \sigma_1}, & \Psi &= \frac{\phi - \phi_1}{\phi_b - \phi_1}, \\ \eta &= \frac{r^2}{R^2}, & \xi &= \frac{z}{R}. \end{aligned} \quad (2.8)$$

With the help of these above transformations, (2.1) is identically satisfied and (2.2) to (2.6) take the following forms:

$$\begin{aligned} \eta f^{(IV)} + 2f''' + \frac{\text{Re}}{(1+K)}(ff''' - f'f'') + \frac{K}{8(1+K)\sqrt{\eta}}\left(4\eta M'' + 4M' - \frac{M}{\eta}\right) &= 0, \\ \eta g'' + g' + \frac{\text{Re}}{(1+K)}(fg' - f'g) + \frac{K}{(1+K)}\sqrt{\eta}\left(4N' + \frac{2N}{\eta}\right) &= 0, \\ 4\eta h'' + 4h' - \frac{h}{\eta} + \frac{\text{Re}}{(1+K)}\left(4fh' + \frac{2fh}{\eta}\right) &= 0, \\ 4\eta M'' + 4M' - \frac{M}{\eta} - \frac{4\text{Re}}{\Lambda}(fM' + f'M) - \frac{2K\delta}{\Lambda}(M + \sqrt{\eta}f'') &= 0, \\ 4\eta N'' + 4N' - \frac{N}{\eta} - \frac{2K\delta}{\Lambda}(N + \sqrt{\eta}g') - \frac{4\text{Re}}{\Lambda}(fN' + Mg) &= 0, \\ \eta\theta'' + \theta' + \text{Pr Re } f\theta' + N_b\eta\theta'\Psi' + N_t\eta\theta'^2 &= 0, \\ \eta\Psi'' + \Psi' + \text{Le Pr Re } f\Psi' + \frac{N_t}{N_b}(\eta\theta'' + \theta') &= 0, \end{aligned} \quad (2.9)$$

where  $\text{Re} = UR/2\nu$  is the cross-flow Reynolds number,  $\text{Pr} = \nu/\alpha$  is the Prandtl number,  $\Lambda = \gamma/\mu j$  is the micropolar coefficient,  $\delta = R^2/j$  and  $K = k^*/\mu$  are the micropolar parameters,  $\text{Le} = \alpha/D_B$  is the Lewis number,  $N_b = \rho^*c_p^*D_B(\phi_b - \phi_1)/\rho c_p\alpha$  is the Brownian motion parameter, and  $N_t = \rho^*c_p^*D_T(\sigma_b - \sigma_1)/\rho c_p\alpha\sigma_1$  is the thermophoresis parameter.

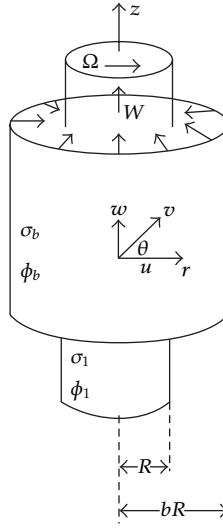


**Figure 1:** The inner cylinder is rotating with angular velocity  $\Omega$  and move axially with velocity  $W$ . The outer cylinder is fixed with fluid injected towards the inner cylinder.

The boundary conditions in nondimensional form are

$$\begin{aligned}
 f(1) &= 0, & f'(1) &= 0, & f(b) &= \sqrt{b}, & f'(b) &= 0, \\
 g(1) &= 1, & g(b) &= 0, & h(1) &= 1, & h(b) &= 0, \\
 M(1) &= -2nf''(1), & M(b) &= 0, & N(1) &= -2ng'(1), & N(b) &= 0, \\
 \theta(1) &= 0, & \theta(b) &= 1, & \Psi(1) &= 0, & \Psi(b) &= 1.
 \end{aligned} \tag{2.10}$$

### 3. Solution of the Problem

The solution of the above boundary value problem is obtained with the help of HAM. For HAM solution we choose the initial guesses as [17–23]

$$\begin{aligned}
 f_0(\eta) &= \frac{\sqrt{b}}{b-1} \left( (3b-1) - 6b\eta + 3(b+1)\eta^2 - 2\eta^3 \right), \\
 g_0(\eta) &= \frac{b-\eta}{b-1}, & h_0(\eta) &= \frac{b-\eta}{b-1}, \\
 M_0(\eta) &= \frac{-6\sqrt{b}n}{(b-1)^3} (b-\eta), & N_0(\eta) &= \frac{2n}{(b-1)^2} (b-\eta), \\
 \theta_0(\eta) &= \frac{\eta-1}{b-1}, & \Psi_0(\eta) &= \frac{\eta-1}{b-1}.
 \end{aligned} \tag{3.1}$$

The corresponding auxiliary linear operators are

$$\begin{aligned} L_f &= \frac{d^4}{d\eta^4}, & L_g &= \frac{d^2}{d\eta^2}, & L_h &= \frac{d^2}{d\eta^2}, \\ L_M &= \frac{d^2}{d\eta^2}, & L_N &= \frac{d^2}{d\eta^2}, & L_\theta &= \frac{d^2}{d\eta^2}, \\ & & L_\Psi &= \frac{d^2}{d\eta^2}. \end{aligned} \quad (3.2)$$

These operators satisfy

$$\begin{aligned} L_f [c_1 + c_2\eta + c_3\eta^2 + c_4\eta^3] &= 0, \\ L_g [c_5 + c_6\eta] &= 0, & L_h [c_7 + c_8\eta] &= 0, \\ L_M [c_9 + c_{10}\eta] &= 0, & L_N [c_{11} + c_{12}\eta] &= 0, \\ L_\theta [c_{13} + c_{14}\eta] &= 0, & L_\Psi [c_{15} + c_{16}\eta] &= 0, \end{aligned} \quad (3.3)$$

where  $c_i$  ( $i = 1, \dots, 16$ ) are arbitrary constants. The zeroth-order deformation equations are defined as

$$\begin{aligned} (1-q)L_f [\hat{f}(\eta; q) - f_0(\eta)] &= q\hbar_1 N_f [\hat{f}(\eta; q)], \\ (1-q)L_g [\hat{g}(\eta; q) - g_0(\eta)] &= q\hbar_2 N_g [\hat{g}(\eta; q)], \\ (1-q)L_h [\hat{h}(\eta; q) - h_0(\eta)] &= q\hbar_3 N_h [\hat{h}(\eta; q)], \\ (1-q)L_M [\hat{M}(\eta; q) - M_0(\eta)] &= q\hbar_4 N_M [\hat{M}(\eta; q)], \\ (1-q)L_N [\hat{N}(\eta; q) - N_0(\eta)] &= q\hbar_5 N_N [\hat{N}(\eta; q)], \\ (1-q)L_\theta [\hat{\theta}(\eta; q) - \theta_0(\eta)] &= q\hbar_6 N_\theta [\hat{\theta}(\eta; q)], \\ (1-q)L_\Psi [\hat{\Psi}(\eta; q) - \Psi_0(\eta)] &= q\hbar_7 N_\Psi [\hat{\Psi}(\eta; q)], \end{aligned} \quad (3.4)$$

where

$$\begin{aligned} N_f [\hat{f}(\eta; p)] &= (1+K) (\eta \hat{f}^{iv} + 2\hat{f}''') + \text{Re} (\hat{f} \hat{f}''' - \hat{f}' \hat{f}''') + \frac{K}{8\sqrt{\eta}} \left( 4\eta \hat{M}'' + 4\hat{M}' - \frac{\hat{M}}{\eta} \right), \\ N_g [\hat{g}(\eta; p)] &= (1+K) (\eta \hat{g}'' + \hat{g}') + \text{Re} (\hat{f} \hat{g}' - \hat{f}' \hat{g}) + \frac{K}{4\sqrt{\eta}} \left( 2\hat{N}' + \frac{\hat{N}}{\eta} \right), \end{aligned}$$

$$\begin{aligned}
N_h[\widehat{h}(\eta; p)] &= (1 + K) \left( 4\eta\widehat{h}'' + 4\widehat{h}' - \frac{\widehat{h}}{\eta} \right) + \text{Re} \left( 4\widehat{f}\widehat{h}' + \frac{2\widehat{f}\widehat{h}}{\eta} \right), \\
N_M[\widehat{M}(\eta; p)] &= \Lambda \left( 4\eta\widehat{M}'' + 4\widehat{M}' - \frac{\widehat{M}}{\eta} \right) - 2K\delta(\widehat{M} + \sqrt{\eta}\widehat{f}'') - 4\text{Re}(\widehat{f}\widehat{M}' + \widehat{f}'\widehat{M}), \\
N_N[\widehat{N}(\eta; p)] &= \Lambda \left( 4\eta\widehat{N}'' + 4\widehat{N}' - \frac{\widehat{N}}{\eta} \right) - 2K\delta(\widehat{N} + \sqrt{\eta}\widehat{g}') - 4\text{Re}(\widehat{f}\widehat{N}' + \widehat{M}\widehat{g}), \\
N_\theta[\widehat{\theta}(\eta; q)] &= \eta\widehat{\theta}'' + \widehat{\theta}' + \text{Pr} \text{Re} \widehat{f}\widehat{\theta}' + N_b\eta\widehat{\theta}'\widehat{\Psi}' + N_t\eta\widehat{\theta}^2, \\
N_\Psi[\widehat{\Psi}(\eta; q)] &= \eta\widehat{\Psi}'' + \widehat{\Psi}' + \text{Le} \text{Pr} \text{Re} \widehat{f}\widehat{\Psi}' + \frac{N_t}{N_b}(\eta\widehat{\theta}'' + \widehat{\theta}').
\end{aligned} \tag{3.5}$$

The boundary conditions for the zeroth-order system are

$$\begin{aligned}
\widehat{f}(1; q) = 0, \quad \widehat{f}'(1; q) = 0, \quad \widehat{f}(b; q) = \sqrt{b}, \quad \widehat{f}'(b; q) = 0, \\
\widehat{g}(1; q) = 1, \quad \widehat{g}(b; q) = 0, \quad \widehat{h}(1; q) = 1, \quad \widehat{h}(b; q) = 0, \\
\widehat{M}(1; q) = -2nf_0''(1), \quad \widehat{M}(b; q) = 0, \quad \widehat{N}(1; q) = 2ng_0'(1), \quad \widehat{N}(b; q) = 0, \\
\widehat{\theta}(1; q) = 0, \quad \widehat{\theta}(b; q) = 1, \quad \widehat{\Psi}(1; q) = 0, \quad \widehat{\Psi}(b; q) = 1.
\end{aligned} \tag{3.6}$$

The  $m$ th-order deformation equations can be obtained by differentiating the zeroth-order deformation equations (3.4) and the boundary conditions (3.6),  $m$ -times with respect to  $q$ , then dividing by  $m!$ , and finally setting  $q = 0$ , we get

$$\begin{aligned}
L_f[f_m(\eta) - \chi_m f_{m-1}(\eta)] &= \hbar_1 R_{mf}(\eta), \\
L_g[g_m(\eta) - \chi_m g_{m-1}(\eta)] &= \hbar_2 R_{mg}(\eta), \\
L_h[h_m(\eta) - \chi_m h_{m-1}(\eta)] &= \hbar_3 R_{mh}(\eta), \\
L_M[M_m(\eta) - \chi_m M_{m-1}(\eta)] &= \hbar_4 R_{mM}(\eta), \\
L_N[N_m(\eta) - \chi_m N_{m-1}(\eta)] &= \hbar_5 R_{mN}(\eta), \\
L_\theta[\theta_m(\eta) - \chi_m \theta_{m-1}(\eta)] &= \hbar_6 R_{m\theta}(\eta), \\
L_\Psi[\Psi_m(\eta) - \chi_m \Psi_{m-1}(\eta)] &= \hbar_7 R_{m\Psi}(\eta), \\
f_m(1) = 0, \quad f_m'(1) = 0, \quad f_m(b) = 0, \quad f_m'(b) = 0, \\
g_m(1) = 0, \quad g_m(b) = 0, \quad h_m(1) = 0, \quad h_m(b) = 0, \\
M_m(1) = 0, \quad M_m(b) = 0, \quad N_m(1) = 0, \quad N_m(b) = 0, \\
\theta_m(1) = 0, \quad \theta_m(b) = 0, \quad \Psi_m(1) = 0, \quad \Psi_m(b) = 0,
\end{aligned} \tag{3.7}$$

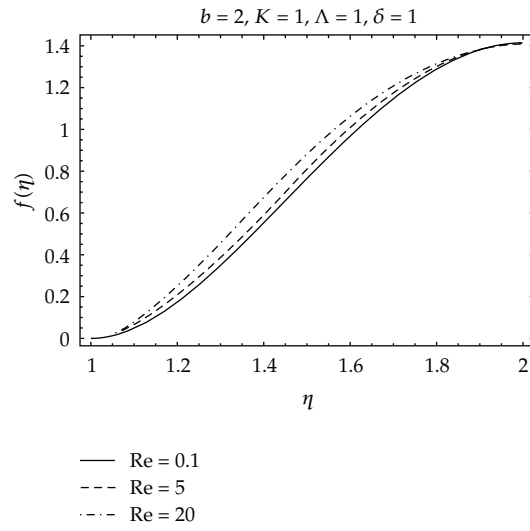


**Figure 2:** Influence of  $Re$  over  $f$  for  $n = 1/2$ .

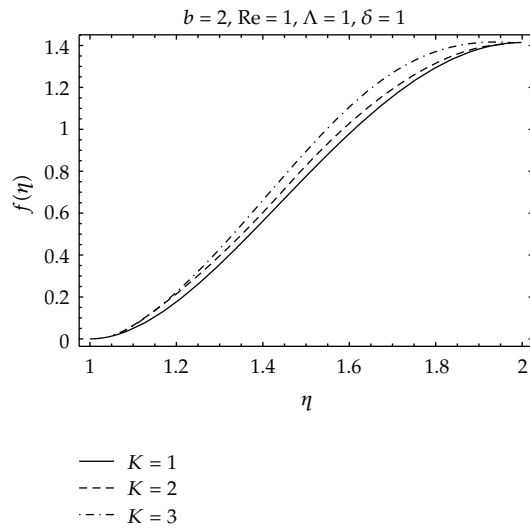


**Figure 3:** Influence of  $K$  over  $f$  for  $n = 1/2$ .

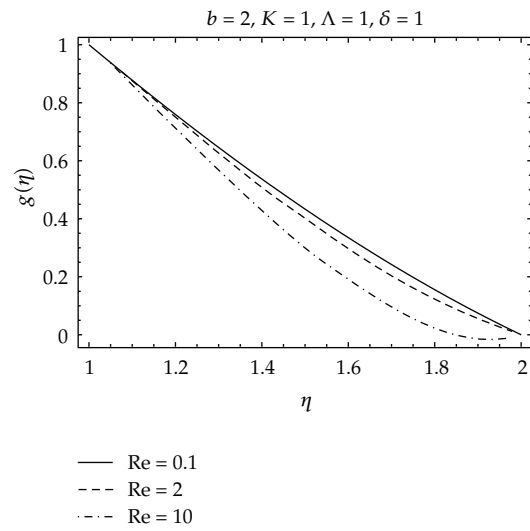


**Figure 4:** Influence of Re over  $g$  for  $n = 1/2$ .

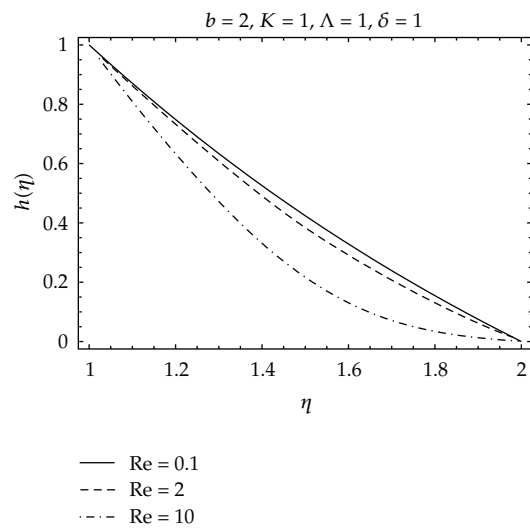


**Figure 5:** Influence of Re over  $h$  for  $n = 1/2$ .



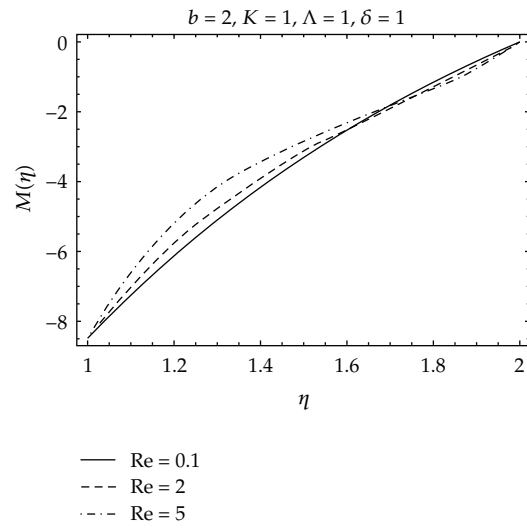


Figure 6: Influence of Re over  $M$  for  $n = 1/2$ .

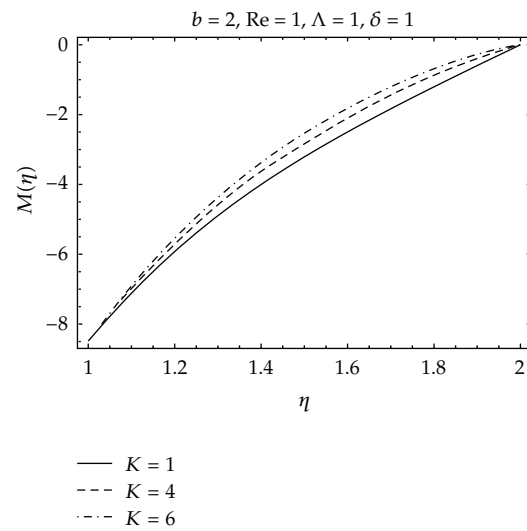
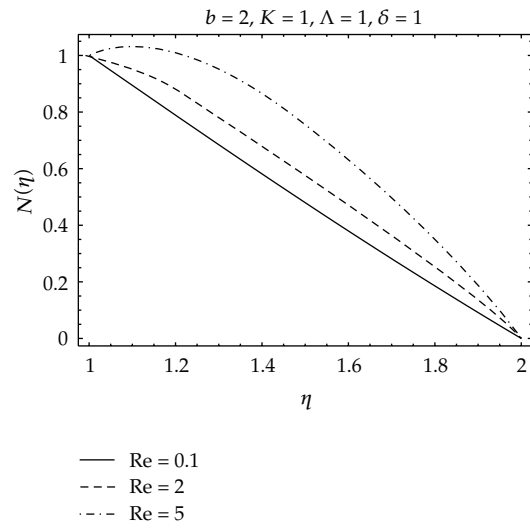
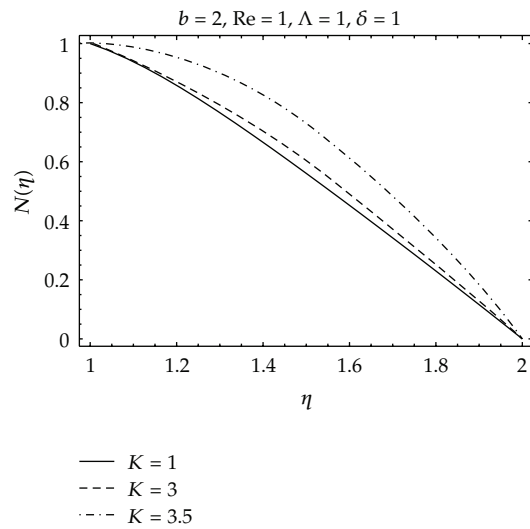


Figure 7: Influence of  $K$  over  $M$  for  $n = 1/2$ .



**Figure 8:** Influence of Re over  $N$  for  $n = 1/2$ .



**Figure 9:** Influence of  $K$  over  $N$  for  $n = 1/2$ .

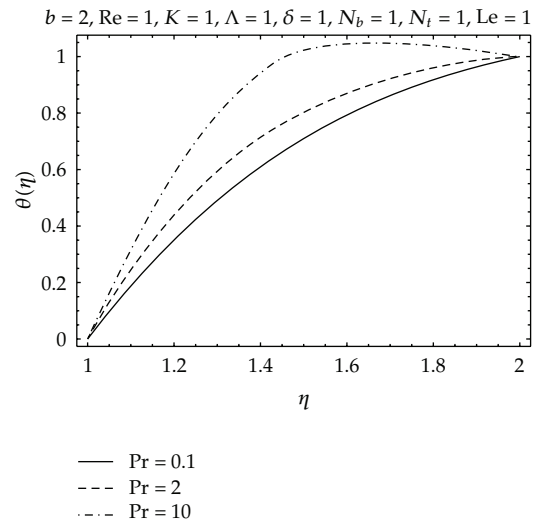


Figure 10: Influence of Pr over  $\theta$  for  $n = 0$ .

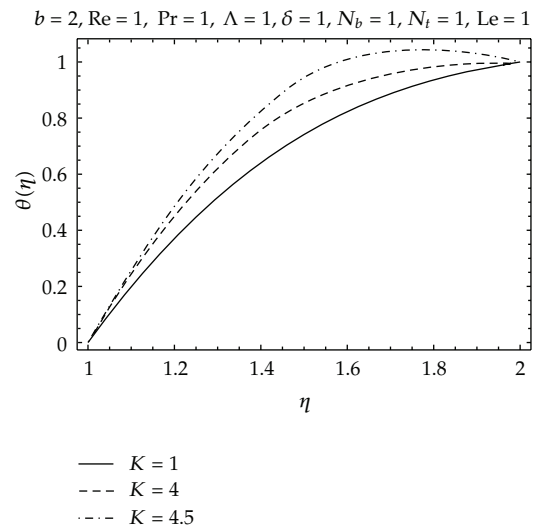
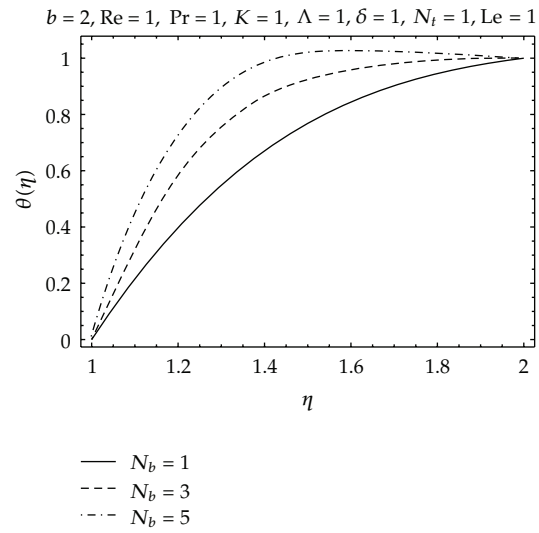
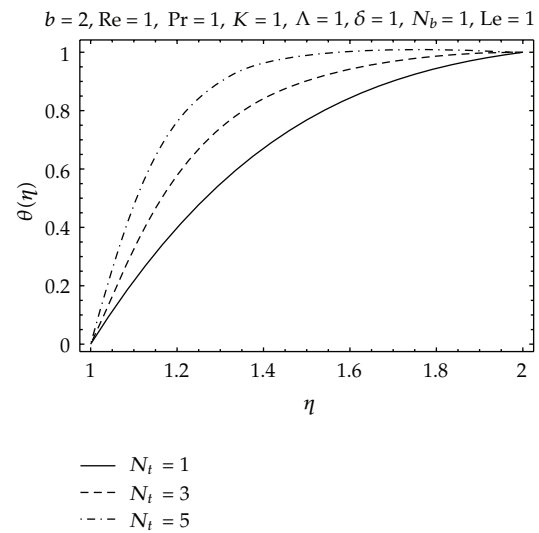


Figure 11: Influence of K over  $\theta$  for  $n = 0$ .



**Figure 12:** Influence of  $N_b$  over  $\theta$  for  $n = 0$ .



**Figure 13:** Influence of  $N_t$  over  $\theta$  for  $n = 0$ .

where

$$\begin{aligned}
 R_{mf}(\eta) &= \eta f'''_{m-1} + 2f'''_{m-1} + \frac{\text{Re}}{1+K} \sum_{j=0}^m (f_j f'''_{m-1-j} - f'_j f''_{m-1-j}) \\
 &\quad + \frac{K}{8(1+K)\sqrt{\eta}} \left( 4\eta M''_{m-1} + 4M'_{m-1} - \frac{M_{m-1}}{\eta} \right), \\
 R_{mg}(\eta) &= \eta g''_{m-1} + g'_{m-1} + \frac{\text{Re}}{1+K} \sum_{j=0}^m (f_j g'_{m-1-j} - f'_j g_{m-1-j}) \\
 &\quad + \frac{K}{1+K} \sqrt{\eta} \left( 4N'_{m-1} + \frac{2}{\eta} N_{m-1} \right), \\
 R_{mh}(\eta) &= 4\eta^2 h''_{m-1} + 4\eta h'_{m-1} - h_{m-1} + \frac{\text{Re}}{1+K} \sum_{j=0}^m (4\eta f_j h'_{m-1-j} + 2f_j h_{m-1-j}), \\
 R_{mM}(\eta) &= 4\eta M''_{m-1} + 4M'_{m-1} - \frac{M_{m-1}}{\eta} - \frac{4\text{Re}}{\Lambda} \sum_{j=0}^m (f_j M'_{m-1-j} + f'_j M_{m-1-j}) \\
 &\quad - \frac{2K\delta}{\Lambda} (M_{m-1} + \sqrt{\eta} f''_{m-1}), \\
 R_{mN}(\eta) &= 4\eta N''_{m-1} + 4N'_{m-1} - \frac{N_{m-1}}{\eta} - \frac{4\text{Re}}{\Lambda} \sum_{j=0}^m (f_j N'_{m-1-j} + M_j g_{m-1-j}) \\
 &\quad - \frac{2K\delta}{\Lambda} (N_{m-1} + \sqrt{\eta} g'_{m-1}), \\
 R_{m\theta}(\eta) &= \eta \theta''_{m-1} + \theta'_{m-1} + \text{Pr} \text{Re} \sum_{j=0}^m f_j \theta'_{m-1-j} + N_b \eta \sum_{j=0}^m \theta'_j \Psi'_{m-1-j} + N_t \eta \sum_{j=0}^m \theta'_j \theta'_{m-1-j}, \\
 R_{m\Psi}(\eta) &= \eta \Psi''_{m-1} + \Psi'_{m-1} + \text{Le Pr} \text{Re} \sum_{j=0}^m f_j \Psi'_{m-1-j} + \frac{N_t}{N_b} (\eta \theta''_{m-1} + \theta'_{m-1}), \\
 \chi_m &= \begin{cases} 0, & m \leq 1, \\ 1, & m > 1. \end{cases}
 \end{aligned}$$

(3.8)

With the help of MATHEMATICA, the solutions of (2.9) subject to the boundary conditions (2.10) can be written as

$$\begin{aligned}
 f(\eta) &= \lim_{Q \rightarrow \infty} \left[ \sum_{m=1}^Q f_m(\eta) \right], & g(\eta) &= \lim_{Q \rightarrow \infty} \left[ \sum_{m=1}^Q g_m(\eta) \right], \\
 h(\eta) &= \lim_{Q \rightarrow \infty} \left[ \sum_{m=1}^Q h_m(\eta) \right], & M(\eta) &= \lim_{Q \rightarrow \infty} \left[ \sum_{m=1}^Q M_m(\eta) \right],
 \end{aligned}$$

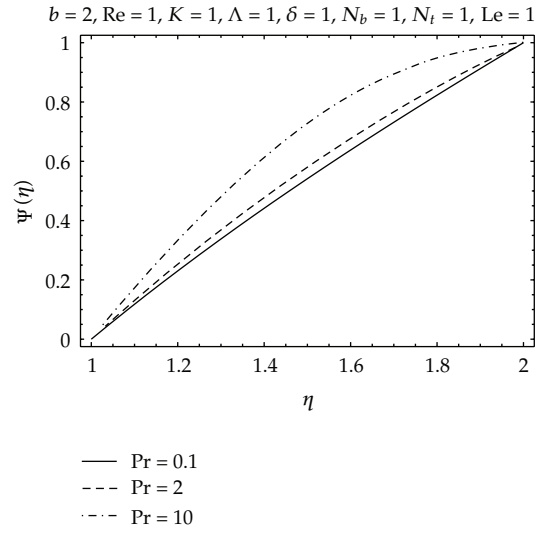


**Figure 14:** Influence of Pr over  $\Psi$  for  $n = 0$ .

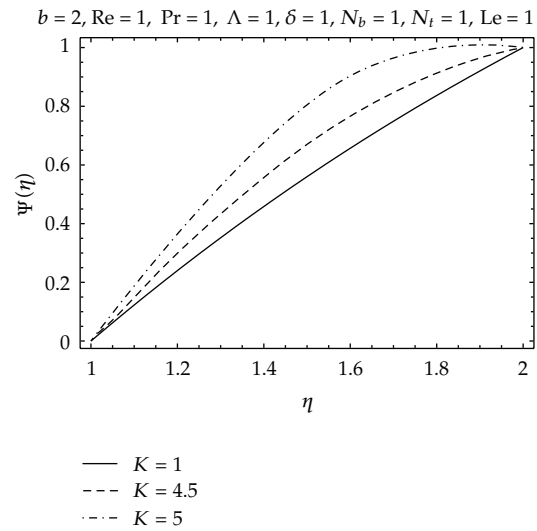


**Figure 15:** Influence of K over  $\Psi$  for  $n = 0$ .

$$N(\eta) = \lim_{Q \rightarrow \infty} \left[ \sum_{m=1}^Q N_m(\eta) \right], \quad \theta(\eta) = \lim_{Q \rightarrow \infty} \left[ \sum_{m=1}^Q \theta_m(\eta) \right],$$

$$\Psi(\eta) = \lim_{Q \rightarrow \infty} \left[ \sum_{m=1}^Q \Psi_m(\eta) \right],$$

(3.9)

where

$$\begin{aligned}
 f_m(\eta) &= f_m^*(\eta) + C_1 + C_2\eta + C_3\eta^2 + C_4\eta^3, \\
 g_m(\eta) &= g_m^*(\eta) + C_5 + C_6\eta, & h_m(\eta) &= h_m^*(\eta) + C_7 + C_8\eta, \\
 M_m(\eta) &= M_m^*(\eta) + C_9 + C_{10}\eta, & N_m(\eta) &= N_m^*(\eta) + C_{11} + C_{12}\eta, \\
 \theta_m(\eta) &= \theta_m^*(\eta) + C_{13} + C_{14}\eta, & \Psi_m(\eta) &= \Psi_m^*(\eta) + C_{15} + C_{16}\eta.
 \end{aligned} \tag{3.10}$$

In which  $f_m^*(\eta)$ ,  $g_m^*(\eta)$ ,  $h_m^*(\eta)$ ,  $M_m^*(\eta)$ ,  $N_m^*(\eta)$ ,  $\theta_m^*(\eta)$ , and  $\Psi_m^*(\eta)$  are the special solutions, and the solutions can be written as

$$f_m(\eta) = \sum_{n=1}^{\infty} a_{mn}\eta^{4n+3}, \quad g_m(\eta) = \sum_{n=1}^{\infty} b_{mn}\eta^{4n+1}, \tag{3.11}$$

$$h_m(\eta) = \sum_{n=1}^{\infty} c_{mn}\eta^{4n+1}, \tag{3.12}$$

$$M_m(\eta) = \sum_{n=1}^{\infty} d_{mn}\eta^{(11n+1)/2}, \quad N_m(\eta) = \sum_{n=1}^{\infty} e_{mn}\eta^{(11n+1)/2}, \tag{3.13}$$

$$\theta_m(\eta) = \sum_{n=1}^{\infty} r_{mn}\eta^{4n+1}, \quad \Psi_m(\eta) = \sum_{n=1}^{\infty} s_{mn}\eta^{4n+1}. \tag{3.14}$$

#### 4. Results and Discussion

The governing nonlinear partial differential equations of the axisymmetric stagnation flow of micropolar nanofluid in a moving cylinder are simplified by using similarity transformation and then the reduced highly nonlinear-coupled differential equations are solved analytically by the help of homotopy analysis method. The velocity field for different values of  $Re$ , and  $K$  are plotted in Figures 2 to 5. It is observed that  $f$  increases with the increase in the parameters  $Re$ , and  $K$  as (see Figures 2 and 3). The values of  $g$  for different values of  $Re$  are shown in Figure 4. It is observed that the nondimensional velocity  $g$  decreases with an increase in  $Re$ . The nondimensional velocity  $h$  for different values of  $Re$  is plotted in Figure 5. It is depicted that the velocity field decreases with the increase in  $Re$ . The variation of microrotation functions  $M$  and  $N$  for different values of  $Re$  and  $K$  are plotted in Figures 6 to 9. It is observed that for increase in both of these parameters  $M$  increases (see Figures 6 and 7). The change in  $N$  is similar to  $M$  (see Figures 8 and 9). The variation of temperature  $\theta$  for different values of  $Pr$ ,  $K$ ,  $N_b$ , and  $N_t$  are shown in Figures 10, 11, 12, and 13. It is observed from these figures that with an increase in these parameters, the temperature field increases. The variation of the nanoparticle concentration  $\Psi$  for different values of  $Pr$ ,  $K$ ,  $N_t$ , and  $Le$  are shown in Figures 14, 15, 16 and 17. It is observed from these figures that with an increase in all the above-mentioned parameters the concentration increases. Physically, it means that the effect of the Prandtl number, micropolar parameter, thermophoresis parameter, and the Lewis number is to increase the nanoparticle concentration. It may be noted that the temperature and concentration functions are plotted for the case of strong concentration, that is, when  $n = 0$ .

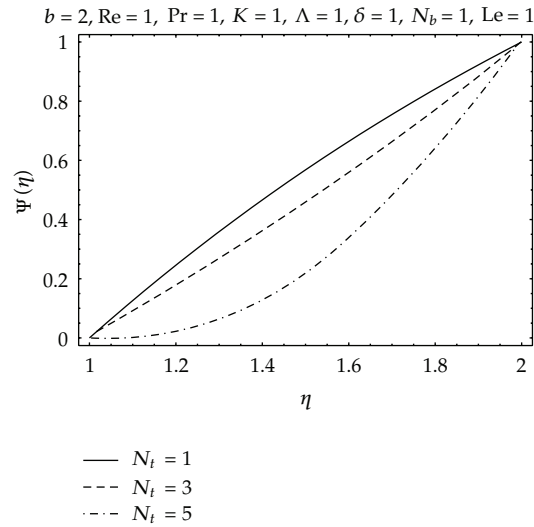


**Figure 16:** Influence of  $N_t$  over  $\Psi$  for  $n = 0$ .

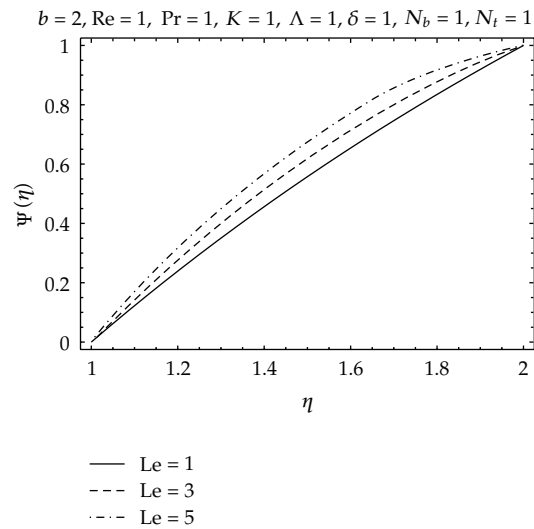


**Figure 17:** Influence of  $Le$  over  $\Psi$  for  $n = 0$ .

## 5. Conclusion

The effects of various physical parameters on the velocity, temperature, and nondimensional nanoparticle parameter are summarized as the following.

- (1) With the increase in Reynold's number  $Re$  the velocity  $f$ , microrotation velocities  $M$  and  $N$ , temperature  $\theta$ , and nanoparticle concentration  $\Psi$  increase, while the velocity profiles for  $g$  and  $h$  decrease.
- (2) With the increase in micropolar parameter  $K$ , the profiles  $f, g, h, M, N, \theta$ , and  $\Psi$  all have shown increasing behavior.



- (3) With the increase in Prandtl number  $Pr$ , the temperature profile  $\theta$  and nanoparticle concentration  $\Psi$  increase.
- (4) With the increase in Brownian motion parameter  $N_b$ , the temperature profile  $\theta$  and nanoparticle concentration  $\Psi$  increase.
- (5) With the increase in thermophoresis parameter  $N_t$ , the temperature profile  $\theta$  and nanoparticle concentration  $\Psi$  increase.
- (6) With the increase in Lewis number  $Le$ , the nanoparticle concentration  $\Psi$  increases.

## Acknowledgment

This paper was supported by WCU (World Class University) Program through the National Research Foundation of Korea (NRF) funded by the Ministry of Education, Science and Technology R31-2008-000-10049-0.

## References

- [1] K. Hiemenz, "Die Grenzschicht an einem in den gleichförmigen Flüssigkeitsstrom eingetauchten geraden Kreiszylinder," *Dingler's Polytechnic Journal*, vol. 326, pp. 321–324, 1911.
- [2] F. Labropulu, D. Li, and I. Pop, "Non-orthogonal stagnation-point flow towards a stretching surface in a non-Newtonian fluid with heat transfer," *International Journal of Thermal Sciences*, vol. 49, no. 6, pp. 1042–1050, 2010.
- [3] Y. Y. Lok, N. Amin, and I. Pop, "Unsteady boundary layer flow of a micropolar fluid near the rear stagnation point of a plane surface," *International Journal of Thermal Sciences*, vol. 42, no. 11, pp. 995–1001, 2003.
- [4] F. Labropulu and D. Li, "Stagnation-point flow of a second-grade fluid with slip," *International Journal of Non-Linear Mechanics*, vol. 43, no. 9, pp. 941–947, 2008.
- [5] R. Nazar, N. Amin, D. Filip, and I. Pop, "Stagnation point flow of a micropolar fluid towards a stretching sheet," *International Journal of Non-Linear Mechanics*, vol. 39, no. 7, pp. 1227–1235, 2004.
- [6] S. Nadeem, A. Hussain, and M. Khan, "HAM solutions for boundary layer flow in the region of the stagnation point towards a stretching sheet," *Communications in Nonlinear Science and Numerical Simulation*, vol. 15, no. 3, pp. 475–481, 2010.
- [7] A. Ishak, R. Nazar, N. Bachok, and I. Pop, "MHD mixed convection flow near the stagnation-point on a vertical permeable surface," *Physica A*, vol. 389, no. 1, pp. 40–46, 2010.
- [8] A. Ishak, K. Jafar, R. Nazar, and I. Pop, "MHD stagnation point flow towards a stretching sheet," *Physica A*, vol. 388, no. 17, pp. 3377–3383, 2009.
- [9] A. Ishak, R. Nazar, and I. Pop, "Stagnation flow of a micropolar fluid towards a vertical permeable surface," *International Communications in Heat and Mass Transfer*, vol. 35, no. 3, pp. 276–281, 2008.
- [10] F. Labropulu and M. Chinichian, "Unsteady oscillatory stagnation-point flow of a viscoelastic fluid," *International Journal of Engineering Science*, vol. 42, no. 7, pp. 625–633, 2004.
- [11] M. H. Haroun, "Non-linear peristaltic flow of a fourth grade fluid in an inclined asymmetric channel," *Computational Materials Science*, vol. 39, no. 2, pp. 324–333, 2007.
- [12] A. C. Eringen, "Theory of micropolar fluids," *The Journal of Mathematical Fluid Mechanics*, vol. 16, pp. 1–18, 1966.
- [13] W. A. Khan and I. Pop, "Boundary-layer flow of a nanofluid past a stretching sheet," *International Journal of Heat and Mass Transfer*, vol. 53, no. 11–12, pp. 2477–2483, 2010.
- [14] S. U. S. Choi, "Enhancing thermal conductivity of fluids with nanoparticles," in *Proceedings of the ASME International Mechanical Engineering Congress and Exposition*, vol. 231, pp. 99–105, American Society of Mechanical Engineers, Fluids Engineering Division, San Francisco, Calif, USA, November 1995.
- [15] A. V. Kuznetsov and D. A. Nield, "Natural convective boundary-layer flow of a nanofluid past a vertical plate," *International Journal of Thermal Sciences*, vol. 49, no. 2, pp. 243–247, 2010.
- [16] L. Hong and C. Y. Wang, "Annular axisymmetric stagnation flow on a moving cylinder," *International Journal of Engineering Science*, vol. 47, no. 1, pp. 141–152, 2009.

- [17] S. J. Liao, *Beyond Perturbation: Introduction to the Homotopy Analysis Method*, Chapman & Hall/CRC Press, Boca Raton, Fla, USA, 2003.
- [18] S. Liao, "Notes on the homotopy analysis method: some definitions and theorems," *Communications in Nonlinear Science and Numerical Simulation*, vol. 14, no. 4, pp. 983–997, 2009.
- [19] S. Nadeem and N. S. Akbar, "Influence of heat transfer on a peristaltic flow of Johnson Segalman fluid in a non uniform tube," *International Communications in Heat and Mass Transfer*, vol. 36, no. 10, pp. 1050–1059, 2009.
- [20] S. Nadeem and N. S. Akbar, "Effects of temperature dependent viscosity on peristaltic flow of a Jeffrey-six constant fluid in a non-uniform vertical tube," *Communications in Nonlinear Science and Numerical Simulation*, vol. 15, no. 12, pp. 3950–3964, 2010.
- [21] A. K. Alomari, M. S. M. Noorani, R. Nazar, and C. P. Li, "Homotopy analysis method for solving fractional Lorenz system," *Communications in Nonlinear Science and Numerical Simulation*, vol. 15, no. 7, pp. 1864–1872, 2010.
- [22] S. Nadeem, T. Hayat, S. Abbasbandy, and M. Ali, "Effects of partial slip on a fourth-grade fluid with variable viscosity: an analytic solution," *Nonlinear Analysis: Real World Applications*, vol. 11, no. 2, pp. 856–868, 2010.
- [23] A. K. Alomari, M. S. M. Noorani, and R. Nazar, "On the homotopy analysis method for the exact solutions of Helmholtz equation," *Chaos, Solitons & Fractals*, vol. 41, no. 4, pp. 1873–1879, 2009.



# Hindawi

Submit your manuscripts at  
<http://www.hindawi.com>

